

# Electroanalytical Performance of Carbon Films with Near-Atomic Flatness

Srikanth Ranganathan and Richard L. McCreery\*

Department of Chemistry, The Ohio State University, 100 West 18th Avenue, Columbus, Ohio 43210-1185

**Physicochemical and electrochemical characterization of carbon films obtained by pyrolyzing a commercially available photoresist has been performed. Photoresist spin-coated on to a silicon wafer was pyrolyzed at 1000 °C in a reducing atmosphere (95% nitrogen and 5% hydrogen) to produce conducting carbon films. The pyrolyzed photoresist films (PPF) show unusual surface properties compared to other carbon electrodes. The surfaces are nearly atomically smooth with a root-mean-square roughness of <0.5 nm. PPF have a very low background current and oxygen/carbon atomic ratio compared to conventional glassy carbon and show relatively weak adsorption of methylene blue and anthraquinone-2,6-disulfonate. The low oxygen/carbon ratio and the relative stability of PPF indicate that surfaces may be partially hydrogen terminated. The pyrolyzed films were compared to glassy carbon (GC) heat treated under the same conditions as pyrolysis to evaluate the electroanalytical utility of PPF. Heterogeneous electron-transfer kinetics of various redox systems were evaluated. For  $\text{Ru}(\text{NH}_3)_6^{3+/2+}$ ,  $\text{Fe}(\text{CN})_6^{3-/4-}$ , and chlorpromazine, fresh PPF surfaces show electron-transfer rates similar to those on GC, but for redox systems such as  $\text{Fe}^{3+/2+}$ , ascorbic acid, dopamine, and oxygen, the kinetics on PPF are slower. Very weak interactions between the PPF surface and these redox systems lead to their slow electron-transfer kinetics. Electrochemical anodization results in a simultaneous increase in background current, adsorption, and electron-transfer kinetics. The PPF surfaces can be chemically modified via diazonium ion reduction to yield a covalently attached monolayer. Such a modification could help in the preparation of low-cost, high-volume analyte-specific electrodes for diverse electroanalytical applications. Overall, pyrolysis of the photoresist yields an electrode surface with properties similar to a very smooth version of glassy carbon, with some important differences in surface chemistry.**

Carbon is a commonly used solid electrode material due to its wide potential window, low cost, mechanical stability, and applicability to a wide range of redox systems. Several reviews are available discussing its utility in electroanalytical chemistry,

electrosynthesis, energy storage, and energy conversion.<sup>1–5</sup> Microfabrication of low-cost and disposable electrodes has received attention recently due to the development of electrochemical sensors.<sup>6–8</sup> Of particular interest are the thick-film screen-printed carbon electrodes prepared using commercially available carbon inks,<sup>8–13</sup> and a majority of the glucose sensors currently available use such electrodes.<sup>8</sup> A review on the applications of screen-printed carbon electrodes in sensing a variety of species including glucose and toxic metal ions has been published.<sup>8</sup> Carbon inks contain a mixture of graphite particles, a binding polymer, and other materials including adhesion promoters. They are available from different manufacturers with varying composition, which is usually proprietary. They differ significantly in their electron-transfer kinetics, as reported by Wang et al.<sup>9</sup> Hence, the general analytical value of these materials also varies. We propose the carbon films prepared by pyrolyzing photoresist as a simple alternative to these thick-film electrodes. The use of photoresist in integrated circuit industry for microfabrication is well known. The established technique of microfabrication using photoresist can also help in the preparation of patterned electrodes of different sizes and shapes. They have a potential to be used in microelectromechanical systems, batteries, capacitors, etc. A simple interdigitated pattern of carbon electrodes combines the advantages of carbon electrodes with the advantages of a microelectrode array. Arrays of microelectrodes have significant advantages over conventionally sized electrodes due to higher signal-to-background ratio and lower detection limits. Interdigitated carbon electrodes prepared by other means have been evaluated for electrochemical

- (1) Kinoshita, K. *Carbon: Electrochemical and Physicochemical Properties*; Wiley: New York, 1988.
- (2) McCreery, R. L. In *Electroanalytical Chemistry*; Bard, A. J., Ed.; Dekker: New York, 1991; Vol.17, pp 221–374.
- (3) McCreery, R. L. In *Laboratory Techniques in Electroanalytical Chemistry*, 2nd ed.; Kissinger, P. T., Heineman, W. R., Eds.; Dekker: New York, 1996; Chapter 10.
- (4) McCreery, R. L. In *Interfacial Electrochemistry*; Wieckowski, A., Ed.; Dekker: New York, 1999; Chapter 35.
- (5) McCreery, R. L.; Cline, K. K.; McDermott, C. A.; McDermott, M. T. *Colloids Surf.* **1994**, *93*, 211.
- (6) Alvarez-Icaza, M.; Bilitewski, U. *Anal. Chem.* **1993**, *65*, 525A.
- (7) Lindner, E.; Buck, R. P. *Anal. Chem.* **2000**, *72*, 336A.
- (8) Hart, J. P.; Wring, S. A., *Electroanalysis* **1994**, *6*, 617
- (9) Wang, J.; Tian, B.; Nascimento, V. B.; Angnes, L. *Electrochim. Acta* **1998**, *43* (23), 3459.
- (10) Wang, J.; Tian, B.; Sahlin, E. *Anal. Chem.* **1999**, *71*, 5436.
- (11) Wang, J.; Pedrero, M.; Pamidi, P. V. A.; Cai, X. *Electroanalysis* **1995**, *7* (11), 1032.
- (12) Wang, J.; Pamidi, P. V. A.; Park, D. S. *Anal. Chem.* **1996**, *68*, 2705.
- (13) Wang, J.; Pedrero, M.; Sakslund, H.; Hammerich, O.; Pingarron, J. *Analyst* **1996**, *121*, 345.

\* Corresponding author: (telephone) (614) 292-2021; (fax) (614) 688-5402; (e-mail) mcreery.2@osu.edu.

detection including capillary electrophoresis and liquid chromatography.<sup>14–19</sup> Since the preparation of patterned electrodes by pyrolyzing photoresist is expected to be inexpensive, we can envisage the manufacture of inexpensive, disposable electrodes.

Kinoshita and co-workers first reported the electrochemical properties of pyrolyzed photoresist films,<sup>20</sup> and Ranganathan et al. have described several of their electrochemical properties.<sup>21</sup> In recent reports, the preparation of interdigitated carbon electrodes by pyrolyzing patterned photoresist and their use in iodide reduction were also presented.<sup>22,23</sup> As is the case with most other procedures for preparing carbon films, the surface of PPF has not been thoroughly characterized as far as electrochemical reactivity and related surface properties. Factors such as edge/basal plane ratio, surface oxides, adsorption strength, surface cleanliness, etc., can vary the heterogeneous electron-transfer rate constants of a number of redox systems by orders of magnitude.<sup>4,5,24</sup>

The goal of the current study is characterization of pyrolyzed photoresist films in the context of applications in electroanalytical chemistry. Several approaches used to examine the reactivity of glassy carbon (GC) and graphite electrodes are applied to pyrolyzed photoresist films (PPF) in order to determine their electrochemical characteristics. In this report, surface structure, stability, and electron-transfer reactivity of PPF are studied with several techniques, including atomic force microscopy (AFM), Raman spectroscopy, X-ray photoelectron spectroscopy (XPS), and cyclic voltammetry, and are compared to heat-treated glassy carbon electrodes. PPF surfaces were modified by the electrochemical reduction of aromatic diazonium salts to yield a compact covalently attached monolayer. The results of this study show that PPF has some unusual surface properties that may have significant electroanalytical utility.

## EXPERIMENTAL SECTION

The preparation procedure for pyrolyzed photoresist films has been reported previously.<sup>21</sup> Positive photoresist AZ4330 (Clariant Corp., Somerville, NJ) was spin-coated on to a clean silicon wafer (2 or 3 in.) spinning at 6000 rpm on a spin coater (PWM101, Headway Research Inc., Garland, TX). The spin time was 30 s. Multiple coatings were applied to obtain a final film thickness of 5–6  $\mu\text{m}$ . The spin-coated wafer was soft-baked at 90 °C for 20 min and then cut into approximately 1  $\times$  1.5 cm<sup>2</sup> pieces. Pyrolysis occurred in a tube furnace (Lindberg) fitted with a quartz tube flushed by forming gas (95% N<sub>2</sub> + 5% H<sub>2</sub>) for 20 min at room

temperature. Metal and glass tubing were used between the gas supply and pyrolysis tube, to minimize oxygen contamination. Gas flow continued while the temperature was increased at the rate of 10 °C/min to 1000 °C, held at 1000 °C for 60 min, and then cooled to room temperature. The carrier gas was kept flowing (~100 sccm) until the samples cooled to room temperature. Glassy carbon (Tokai GC 20) plates (~1 cm<sup>2</sup> area) were hand-polished successively in 1-, 0.3-, and 0.05- $\mu\text{m}$  alumina slurries on Buehler microcloth polishing cloth followed by sonication in Nanopure water (Barnstead Nanopure Infinity, Dubuque, IA; resistivity > 17.9 M $\Omega$ -cm). Polished GC samples were sonicated for 10 min in a suspension of activated carbon in 2-propanol (AC/IPA; 1/3 ratio) followed by sonication in Nanopure water.<sup>25</sup> Heat-treated GC (HT GC) was prepared by heating the polished, AC/IPA cleaned GC under the same conditions as photoresist pyrolysis (1000 °C; 60 min). The reproducibility of the electrochemical properties of PPF is indicated in Table 3, with the standard deviation of  $\Delta E_p$  for various redox systems on 10 different PPF samples being in the range of 7–29 mV.

All electrochemical measurements were performed with BAS 100W potentiostat (Bioanalytical Systems, West Lafayette, IN), with an Ag/AgCl reference electrode (BAS) aqueous solutions and Ag/Ag<sup>+</sup> reference electrode (BAS) for acetonitrile solutions. The electrochemical studies were done in a custom-made single-compartment cell made from Teflon with Ag/AgCl as reference and platinum wire as counter electrodes. The working electrode area (0.24 cm<sup>2</sup>) was defined by a viton O-ring, and contact to the working electrode was made from the top of the carbon film using a copper wire. Adhesion of PPF to the substrate was strong, and no damage by the contact wire was observed. Unless mentioned, all electrochemical studies were done on surfaces treated with AC/IPA sonication followed by sonication in Nanopure water. Those electrodes will be referred to as AC/IPA surfaces.<sup>25</sup>

Surface derivatization of PPF was performed using 5 mM solutions of the corresponding diazonium salt in acetonitrile.<sup>26–30</sup> *n*-Tetrabutylammonium tetrafluoroborate (TBABF<sub>4</sub>, 0.1 M; Aldrich) was used as the supporting electrolyte. Tetrafluoroborate salts of 4-nitrophenyl, 4-trifluoromethylphenyl, 4-nitroazobenzene-4', and 2-anthraquinone diazonium ion were prepared as described elsewhere.<sup>27,31</sup> The diazonium salt solutions were degassed with argon for at least 20 min before derivatization. The redox systems studied were as follows: 1 mM Fe<sup>2+</sup> in 0.2 M HClO<sub>4</sub> made from Fe(NH<sub>4</sub>)<sub>2</sub>(SO<sub>4</sub>)<sub>2</sub>·12H<sub>2</sub>O (Mallinckrodt Inc.) and 70% HClO<sub>4</sub> (GFS Chemicals); 1 mM Fe(CN)<sub>6</sub><sup>4-</sup> in 1 M KCl from K<sub>4</sub>Fe(CN)<sub>6</sub> (Mallinckrodt Inc.); 1 and 0.1 mM [Ru(NH<sub>3</sub>)<sub>6</sub>]<sup>3+</sup> in 1 M KCl from Ru(NH<sub>3</sub>)<sub>6</sub>Cl<sub>3</sub> (Aldrich); 1 mM ascorbic acid (AA, Aldrich Chemical Co.) in 0.1 M H<sub>2</sub>SO<sub>4</sub>; 1 mM dopamine (DA, Sigma) in 0.1 M H<sub>2</sub>SO<sub>4</sub>; 1 mM oxygen in 1 M KOH (Mallinckrodt Inc.); and 1 mM chlorpromazine (CPZ, Sigma) in 0.2 M NaCl, 0.01 M HCl, 40% methanol. Other chemicals included the following: sulfuric acid

(14) Tabei, H.; Morita, M.; Niwa, O.; Horiuchi, T. *J. Electroanal. Chem.* **1992**, *334*, 25.

(15) Niwa, O.; Tabei, H. *Anal. Chem.* **1994**, *66*, 285.

(16) Tabei, H.; Takahashi, M.; Hoshino, S.; Niwa, O.; Horiuchi, T. *Anal. Chem.* **1994**, *66*, 3500.

(17) Niwa, O.; Morita, M. *Anal. Chem.* **1996**, *68*, 355.

(18) Liu, Z.; Niwa, O.; Kurita, R.; Horiuchi, T. *Anal. Chem.* **2000**, *72*, 1315.

(19) Fiaccabrino, G. C.; Tang, X.-M.; Skinner, N.; de Rooij, N. F.; Koudelka-Hep, M. *Anal. Chim. Acta* **1996**, *326*, 155.

(20) Kim, J.; Song, X.; Kinoshita, K.; Madou, M.; White, R. *J. Electrochem. Soc.* **1998**, *145*, 2314.

(21) Ranganathan, S.; McCreery, R.; Majji, S. M.; Madou, M. *J. Electrochem. Soc.* **2000**, *147*, 277.

(22) Kostecki, R.; Song, X.; Kinoshita, K. *Electrochem. Solid-State Lett.* **1999**, *2*, 461.

(23) Kostecki, R.; Song, X.; Kinoshita, K. *J. Electrochem. Soc.* **2000**, *147*, 1878.

(24) Chen, P.; McCreery, R. L. *Anal. Chem.* **1996**, *68*, 3958.

(25) Ranganathan, S.; Kuo, T.-C.; McCreery, R. L. *Anal. Chem.* **1999**, *71*, 3574.

(26) Delamar, M.; Hitmi, R.; Pinson, J.; Saveant, J.-M. *J. Am. Chem. Soc.* **1992**, *114*, 5883.

(27) Liu, Y.-C.; McCreery, R. L. *Anal. Chem.* **1997**, *69*, 2091.

(28) Allongue, P.; Delamar, M.; Desbat, B.; Fagebaume, O.; Hitmi, R.; Pinson, J.; Saveant, J.-M. *J. Am. Chem. Soc.* **1997**, *119*, 201.

(29) Delamar, M.; Desarmot, G.; Fagebaume, O.; Hitmi, R.; Pinson, J.; Saveant, J.-M. *Carbon* **1997**, *35*, 801.

(30) Kuo, T.-C.; McCreery, R. L.; Swain, G. M. *Electrochem. Solid-State Lett.* **1999**, *2*, 288.

(31) DuVall, S. H.; McCreery, R. L. *J. Am. Chem. Soc.* **2000**, *122*, 6759-6764.

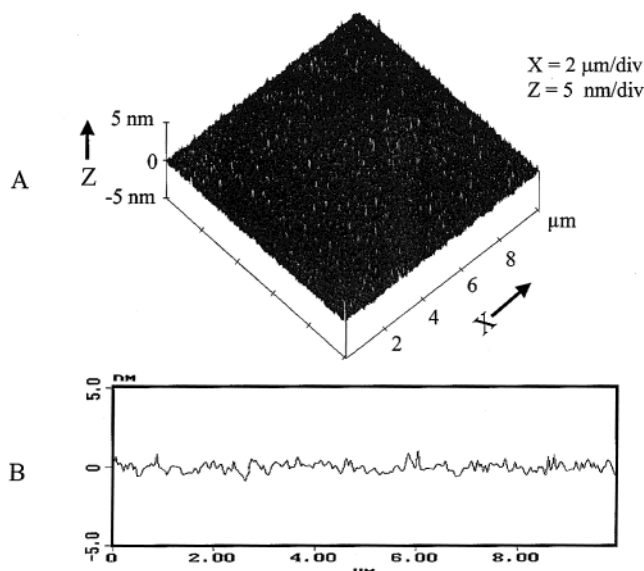


Figure 1. AFM image of a  $10 \times 10 \mu\text{m}$  area of PPF, typical of several locations on a  $1\text{-cm}^2$  sample. Line scan illustrates an rms roughness of 0.5 nm.

(Mallinckrodt Inc.); hydrochloric acid (Fisher Scientific); activated carbon (Darco S-51, Norit Americas Inc.); 2-propanol (IPA, Mallinckrodt Inc.); acetonitrile (ACN, Mallinckrodt Inc.); methanol (Mallinckrodt Inc.); anthraquinone-2,6-disulfonate (AQDS) sodium salt (Aldrich), and methylene blue (MB, Aldrich).

Atomic force microscopy (AFM) was performed with a Nanoscope IIIa Multimode instrument (Digital Instruments, Santa Barbara, CA). Raman spectra were collected in  $180^\circ$  geometry with Ar ion excitation laser (514.5 nm) and  $f/1.5$  spectrograph (Kaiser Holospec) with holographic grating. X-ray photoelectron spectra (XPS) were acquired with a VG Scientific Escalab MKII system with Mg K $\alpha$  X-ray radiation source. All atomic ratios were calculated from the peak areas and were corrected for the sensitivity factors, using the software provided with the instrument.

The adsorption procedure for AQDS, MB, and dopamine has been reported previously.<sup>24,32</sup> A  $10 \mu\text{M}$  solution AQDS in  $0.1 \text{ M HClO}_4$ ,  $10 \mu\text{M}$  solution of MB in  $0.1 \text{ M H}_2\text{SO}_4$ , and a  $10 \mu\text{M}$  solution of dopamine in  $0.1 \text{ M H}_2\text{SO}_4$  were used for the adsorption studies. The electrodes were preadsorbed with the adsorbents by dipping the AC/IPA cleaned surfaces in these solutions for 10 min and then the cyclic voltammograms were taken in a fresh adsorbent solution at a scan rate of  $1 \text{ V/s}$ .

## RESULTS

**Surface Characterization.** The pyrolyzed photoresist films were investigated using AFM, scanning electron microscopy (SEM), transmission electron microscopy (TEM), XPS, Raman spectroscopy, four-point probe resistivity measurements, and thermal gravimetric analysis (TGA). The details and results of some of these studies (TEM, SEM, Raman, TGA, and resistivity) have been reported previously.<sup>21</sup>

**AFM.** Figure 1 shows the tapping mode AFM image of  $10 \mu\text{m} \times 10 \mu\text{m}$  area of a PPF sample and a line profile along a  $10\text{-}\mu\text{m}$  line showing the variation in  $z$ -axis height. The root-mean-square

(rms) roughness along this line is 0.5 nm, and the peak–peak maximum was 1.5 nm. SEM images showed that the PPF surfaces are smooth with no observable features such as pores or defects (note size range). Raman line profiles taken along a  $\sim 900\text{-}\mu\text{m}$  line gave constant intensities of the two characteristic carbon bands, the disorder band at  $\sim 1360 \text{ cm}^{-1}$ , and the graphitic band at  $\sim 1600 \text{ cm}^{-1}$ . Since the microscope focus was maintained along the line, constant intensities indicate an optically smooth surface. AFM images similar to Figure 1 were obtained at random locations on a given PPF sample, and no defects were observed with either AFM or optical microscopy.

Compared to other carbon electrode surfaces, the smoothness of PPF films ( $<0.5 \text{ nm rms}$ ) is exceptional, approaching that of the atomically smooth basal plane HOPG, whose rms roughness determined by STM is  $0.24 \text{ nm}$ .<sup>32</sup> Reported roughness for polished GC ranges from  $4.1 \pm 0.1 \text{ nm}$  from STM<sup>33</sup> to  $44 \pm 6 \text{ nm}$  from AFM.<sup>34</sup> In the integrated circuit industry, the spin-coated resist itself is expected to have a uniformity of  $\pm 5 \text{ nm}$  and a repeatability of  $<1 \text{ nm}$  is required for defect-free submicrometer features.<sup>35</sup> The smoothness of the PPF surface may very well depend on the uniformity of the spin-coated resist. Apparently the pyrolysis procedure is not introducing any defects or pores as is often observed on GC due to gas evolution.<sup>36</sup> The exceptional smoothness of PPF may result from “liquid curing”, in which localized flow of polymer occurs during curing above the glass transition temperature. Combined with the reducing atmosphere to minimize carbon oxidation, the PPF curing process yields a carbon surface approaching the flatness of HOPG or single-crystal metal surfaces.

**XPS.** XPS spectra were obtained immediately upon removal of samples from the pyrolysis furnace. The oxygen/carbon (O/C) atomic ratio for a fresh PPF and HT GC samples are  $2.3 \pm 0.5$  ( $N = 10$ ) and  $1.6 \pm 0.9\%$  ( $N = 10$ ), respectively. For comparison, AC/IPA polished GC samples had an O/C ratio of  $6.7 \pm 0.5\%$  ( $N = 5$ ). The low O/C ratio observed on GC is similar to the values for vacuum heat-treated GC.<sup>24</sup> The presence of hydrogen in the pyrolysis atmosphere presumably reduces the O/C ratio by reacting with the trace oxygen that may be present in the atmosphere and terminating the surface carbon atoms with hydrogen. The reduction in surface oxygen functionalities is also supported by the near elimination of the higher binding energy shoulder in the C 1s peak typically observed on high O/C surfaces. Past research reports significant to this study include the pyrolysis of polymers<sup>37</sup> and hydrogen termination of glassy carbon surfaces.<sup>34,38</sup> Whitesides and co-workers made glassy carbon-like materials by pyrolyzing polymers at  $1000^\circ \text{C}$  in an atmosphere of argon.<sup>37</sup> These materials had a maximum O/C ratio of 8%. Glassy carbon surfaces treated with hydrogen plasma at high temperatures ( $>1000^\circ \text{C}$ ), yielded hydrogen-terminated GC (HGC) with a low O/C ratio (1–4%).<sup>38</sup> This surface is one of the most stable carbon surfaces to air oxidation with a

(32) McDermott, M. T.; Kneten, K. R.; McCreery, R. L. *J. Phys. Chem.* **1992**, *96*, 3124.

(33) McDermott, M. T.; McDermott, C. A.; McCreery, R. L. *Anal. Chem.* **1993**, *65*, 937.

(34) Chen, Q.; Swain, G. M. *Langmuir* **1998**, *14*, 7017.

(35) Madou, M. *Fundamentals of Microfabrication*; CRC Press: New York, 1997.

(36) Ray, K. G.; McCreery, R. L. *Anal. Chem.* **1997**, *69*, 4680–4687.

(37) Schueller, O. J. A.; Brittain, S. T.; Marzolin, C.; Whitesides, G. M. *Chem. Mater.* **1997**, *9*, 1399.

(38) Kuo, T.-C.; McCreery, R. L. *Anal. Chem.* **1999**, *71*, 1553.

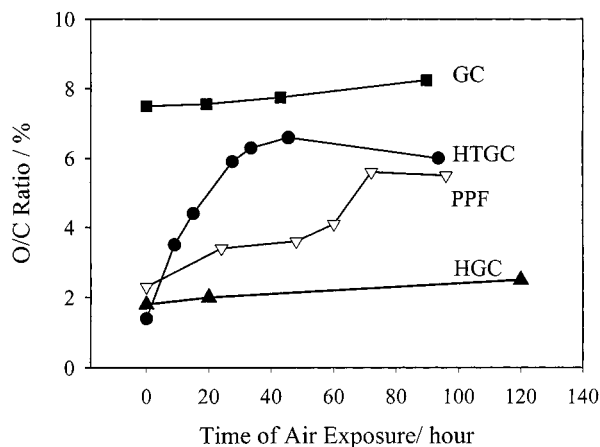


Figure 2. Surface O/C ratios determined from XPS for several carbon surfaces, as a function of exposure time in laboratory air. GC was initially polished and then treated with AC/IPA. HT GC was heated at 1000 °C for 60 min in flowing 95% N<sub>2</sub>/5% H<sub>2</sub>. PPF prepared as described in Experimental Section. HGC is hydrogenated GC data from ref 38.

Table 1. Effect of Potential Cycling in 0.2 M HClO<sub>4</sub> between -0.5 and 1.5 V on Oxygen/Carbon (O/C) Ratio and  $\Delta E_p$  of Fe<sup>3+/2+</sup>

conditions	PPF		HT GC	
	O/C ratio (%)	$\Delta E_p$ of Fe <sup>3+/2+</sup> (mV)	O/C ratio (%)	$\Delta E_p$ of Fe <sup>3+/2+</sup> (mV) <sup>a</sup>
before cycling	3.3	671	1.7	342
after 20 cycles	11.5	629	12.1	287
+20 cycles	16.8	578	18.1	251
+60 cycles	19.7	492	20.6	239

<sup>a</sup> Scan rate, 0.2 V/s.

stable low O/C ratio for extended periods of time. Low oxide carbon surfaces are known to react with atmospheric oxygen, resulting in surfaces with increasing O/C ratio, reaching ~7% within a few hours.<sup>24</sup> The relative stability of PPF and HT GC surfaces toward air oxidation were monitored using the XPS and the results are shown in Figure 2. Both PPF and HT GC are unstable in air, and their O/C ratios increase to values near 5–6% upon exposure to laboratory air. The rates of increase of O/C ratios for PPF and HT GC are slower than the other low oxide surfaces, except for HGC. In comparison to HT GC, the PPF surface appears to be more stable toward air oxidation with its O/C ratio increasing more slowly than HT GC. The stability of hydrogenated GC formed in a hydrogen plasma was attributed to termination of reactive radical sites on the GC surface.<sup>38</sup> On the basis of Figure 2, the PPF surfaces are partly H-terminated, but not as completely as HGC.

The stability of PPF surfaces toward electrochemical oxidation was investigated by electrochemical cycling similar to that reported for HGC.<sup>38</sup> Electrochemical cycling of PPF and HT GC was conducted in 0.2 M HClO<sub>4</sub> between the potential limits -0.5 and +1.5 V, with results tabulated in Table 1. Both PPF and HT GC oxidize as a result of potential cycling, with the O/C ratio increasing with the number of cycles. The table also shows how the increase in surface oxygen functionalities affects the electron-transfer kinetics of the Fe<sup>3+/2+</sup> redox system, which is known to

Table 2. Capacitance, Adsorption, and  $\Delta E_p$  of Dopamine (DA) on Various Carbon Surfaces

	capacitance <sup>a,b</sup> ( $\mu\text{F}/\text{cm}^2$ )	surface coverage <sup>c</sup> of MB (pmol/cm <sup>2</sup> ) <sup>2</sup>	$\Delta E_p$ for DA <sup>a</sup> (mV)
polished GC	40 ± 2	135 ± 23	87 ± 4
AC/IPA polished GC	66 ± 11 <sup>d</sup>	286 ± 27	77 ± 5
AC/IPA HT GC	21.5 ± 0.5	191 ± 47	74 ± 10
PPF (before AC/IPA)	8.1 ± 1.6	<i>e</i>	<i>e</i>
AC/IPA PPF	9.2 ± 1.5	48 ± 5 <sup>f</sup>	287 ± 18
oxidized PPF <sup>g</sup>	104	296	111

<sup>a</sup> Values reported are mean ± standard deviation for  $N \geq 3$  trials except oxidized PPF. Scan rate for  $\Delta E_p$  determination was 0.20 V/s. <sup>b</sup> Measured from background voltammograms in 1 M KCl (20 V/s) at 0.3 V. <sup>c</sup> Electrodes immersed in 10  $\mu\text{M}$  MB for 10 min; MB solution was replaced and voltammogram recorded at 1 V/s. <sup>d</sup> From ref 25. <sup>e</sup> MB adsorption and DA kinetics varied significantly before sample were cleaned with AC/IPA. <sup>f</sup> Includes significant contribution from diffusion. <sup>g</sup> Oxidized in 0.1 M H<sub>2</sub>SO<sub>4</sub> at 1.8 V for 1 min.

be catalyzed by surface carbonyl groups.<sup>39,40</sup> As the number of cycles increases, the surface O/C ratio increases, resulting in faster Fe<sup>3+/2+</sup> kinetics. The PPF surface does not seem to differ significantly from HGC surfaces toward electrochemical oxidation.

**Electrode Capacitance.** The apparent capacitances on various carbon surfaces determined from background voltammograms in 1 M KCl scanned at 20 V/s are listed in Table 2. No effort was made to quantify the true double-layer capacitance and so the reported capacitance values may include the contributions from other sources such as surface faradaic reactions. The AC/IPA pretreatment increases the capacitance of polished GC, probably by removing surface impurities.<sup>25</sup> The capacitance and voltammetric background observed for PPF are significantly lower than those of GC, before or after AC/IPA treatment. PPF capacitance is also less than half that of HT GC, even though the two surfaces have comparable O/C ratios. The smoothness and the low O/C ratio contribute to the low capacitance observed for PPF, but it is also possible that space charge effects cause the low capacitance.<sup>5,41,42</sup> The anomalously low capacitances on cleaved basal plane of highly ordered pyrolytic graphite (HOPG, 0.6–7  $\mu\text{F}/\text{cm}^2$ )<sup>5</sup> and boron-doped diamond (BDD, 6  $\mu\text{F}/\text{cm}^2$ )<sup>43</sup> have been attributed to space charge capacitance in series with the double layer. As of now, there is no direct evidence to prove that this electronic effect is causing the low capacitance on PPF, but low capacitance on PPF may be useful in electroanalytical applications.

**Adsorption on PPF.** Adsorption from a low concentration (10  $\mu\text{M}$ ) of methylene blue (MB) was investigated using cyclic voltammetry.<sup>24,32</sup> MB has been shown to physisorb to carbon surfaces strongly, and its 2-electron, surface-confined redox wave can be used to evaluate the surface coverage.<sup>24</sup> The surface coverage of adsorbed MB was determined from the voltammetric reduction charge (after correcting for the background current) and reported in Table 2. The amount of adsorbed MB follows the trend of capacitance, with the AC/IPA-treated GC and oxidized

(39) Chen, P.; Fryling, M. A.; McCreery, R. L. *Anal. Chem.* **1995**, *67*, 3115.

(40) McDermott, C. A.; Kneten, K. R.; McCreery, R. L. *J. Electrochem. Soc.* **1993**, *140*, 3574.

(41) Gerischer, H. *J. Phys. Chem.* **1985**, *89*, 4249.

(42) Morcos, I.; Yeager, E. *Electrochim. Acta* **1972**, *15*, 257.

(43) Xu, J.; Granger, M. C.; Chen, Q.; Strojek, J. W.; Lister, T. E.; Swain, G. M. *Anal. Chem.* **1997**, *69*, 591A.

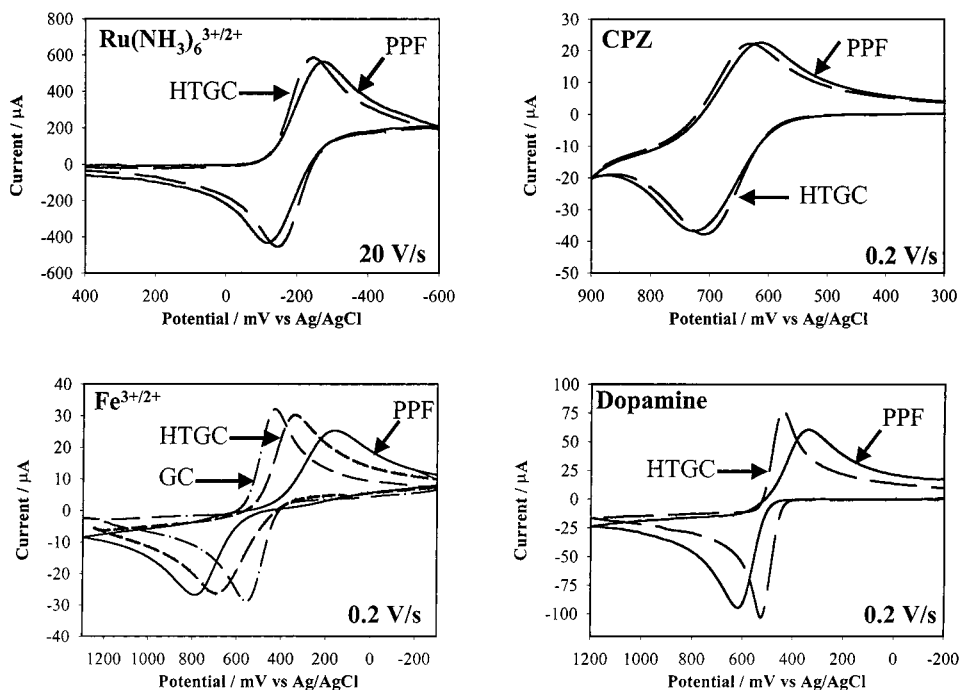


Figure 3. Voltammetry of four redox systems on PPF and heat-treated GC (HT GC). All surfaces were cleaned with activated carbon in IPA before voltammetry. CVs from polished GC were similar to those on HT GC for all redox systems except  $\text{Fe}^{3+/2+}$ , for which the polished GC voltammogram is shown.

Table 3. Electrochemical Results on AC/IPA Heat-Treated GC and AC/IPA Pyrolyzed Photoresist Films

redox system	scan rate (V/s)	$\Delta E_p$ (mV) AC/IPA HT-GC <sup>a</sup>	$\Delta E_p$ (mV) AC/IPA PPF <sup>a</sup> on Si	$\Delta E_p$ (mV) AC/IPA PPF on GC
AA (pH 1) <sup>b</sup>	0.1	304 ± 12 (5)	505 ± 21 (10)	536
DA (pH 1)	0.2	74 ± 10 (5)	287 ± 18 (10)	306
oxygen (pH 14) <sup>c</sup>	0.2	-354 ± 6 (3)	-476 ± 8 (3)	
$\text{Fe}^{3+/2+}$	0.2	297 ± 42 (5)	654 ± 29 (10)	647
$\text{Fe}(\text{CN})_6^{3-/4-}$	20	140 ± 9 (5)	265 ± 17 (10)	240
$\text{Ru}(\text{NH}_3)_6^{3+/2+}$	20	125 ± 5 (5)	222 ± 16 (10)	122
chlorpromazine	0.2	80 ± 2 (5)	109 ± 7 (10)	74

<sup>a</sup> Values in parentheses indicate the number of samples examined. <sup>b</sup>  $E_p^a$  (mV). <sup>c</sup>  $E_p^c$  (mV).

PPF showing the highest values and AC/IPA-treated PPF, the lowest. It should be noted that the reduction wave for MB on AC/IPA-treated PPF has a contribution from diffusing MB, so the observed surface coverage is an overestimate. The adsorption of the anionic adsorbate AQDS is also low on PPF ( $\sim 20$  pmol/cm<sup>2</sup>).

**Electrode Kinetics.** Electron-transfer (ET) kinetics of various redox systems were studied on PPF surfaces and were compared to heat-treated GC. The redox systems were chosen according to their varying sensitivity to carbon surface preparation. Figure 3 compares background-corrected (but no  $iR$  correction) cyclic voltammograms (CV) of  $\text{Ru}(\text{NH}_3)_6^{3+/2+}$ , chlorpromazine,  $\text{Fe}^{3+/2+}$ , and dopamine on PPF with those from HT GC. Figure 3C also shows the CV of  $\text{Fe}^{3+/2+}$  on polished GC. The ET reactivity of HT GC did not differ significantly from polished GC for  $\text{Ru}(\text{NH}_3)_6^{3+/2+}$ , CPZ, or dopamine redox systems, and the results for polished GC are not shown. The PPF shows well-defined, symmetric voltammograms for all the redox systems studied. The  $\Delta E_p$  values are reproducible with a standard deviation of less than 10%. The  $i$  vs  $\nu^{1/2}$  plot for  $\text{Ru}(\text{NH}_3)_6^{3+/2+}$  between the scan rates 0.1 and 20 V/s is linear ( $R^2 > 0.99$ ), indicating currents controlled

by semi-infinite linear diffusion. Other redox systems studied (not shown in the figure) were  $\text{Fe}(\text{CN})_6^{3-/4-}$ , ascorbic acid, and oxygen reduction. The results for all seven redox systems are summarized in Table 3.

Heterogeneous electron-transfer rate constants were calculated for simple 1-electron redox systems using a commercially available simulation program (Digisim, Bioanalytical Systems, West Lafayette, IN). The observed rate constant on PPF for  $\text{Ru}(\text{NH}_3)_6^{3+/2+}$  in 1 M KCl at seven different scan rates is  $0.012 \pm 0.001$  cm/s for 1 mM  $\text{Ru}(\text{NH}_3)_6^{3+/2+}$ , and  $0.025 \pm 0.002$  cm/s for 0.1 mM  $\text{Ru}(\text{NH}_3)_6^{3+/2+}$ . In our previous report, we demonstrated the effects of electrode resistance on the ET kinetics on PPF electrodes.<sup>21</sup> Resistance within the PPF film increases the observed  $\Delta E_p$  value according to

$$(\Delta E_p)_{\text{Corr}} = (\Delta E_p)_{\text{observed}} - 2|iR_u$$

where  $i$  is the peak current in amperes;  $R_u$  is the uncompensated cell resistance that includes the electrode resistance,  $(\Delta E_p)_{\text{observed}}$  is the observed  $\Delta E_p$  in the presence of the uncompensated

Table 4. Heterogeneous Rate Constants ( $k^0$ ) on HT GC and PPF Surfaces

redox system	$k^0_{\text{HTGC}}$ (cm/s) <sup>a</sup>	$k^0_{\text{PPF}}$ (cm/s) <sup>b</sup>	$k^0_{\text{HTGC}}/k^0_{\text{PPF}}$
Fe <sup>3+/2+</sup>	$6.7 \times 10^{-4}$	$2.1 \times 10^{-5}$	32
Fe(CN) <sub>6</sub> <sup>3-/4-</sup>	0.034	0.012	2.8
Ru(NH <sub>3</sub> ) <sub>6</sub> <sup>3+/2+</sup>	0.037	0.020	1.8
chlorpromazine	0.012	0.0054	2.2

<sup>a</sup> Calculated for the mean value reported in Table 3. <sup>b</sup> Calculated rate constant after correcting the mean  $\Delta E_p$  values in Table 3 for PPF resistance.

resistance  $R_0$  in volts, and  $(\Delta E_p)_{\text{corr}}$  is the  $\Delta E_p$  corrected for PPF resistance. Although the resistivity of PPF treated at 1000°C ( $5.7 \times 10^{-3} \Omega \cdot \text{cm}$ ) is only slightly higher than that of Tokai GC 20 ( $(4.0-4.5) \times 10^{-3} \Omega \cdot \text{cm}$ ), the thinness of the PPF film leads to significant internal electrode resistance. On the basis of the film dimensions and resistivity, an internal electrode resistance of 45  $\Omega$  was calculated.

Table 4 compares the ET rate constants (corrected for 45  $\Omega$  of PPF resistance but not for cell resistance) for four 1-electron redox systems on PPF and HT GC. It is well-established that the ET rate constant of Ru(NH<sub>3</sub>)<sub>6</sub><sup>3+/2+</sup> is insensitive to surface chemistry or adsorbed monolayers and thus is considered to be a simple outer-sphere system.<sup>2,4,24</sup> For this redox system, the difference in rate constant between PPF and HT GC is less than a factor of 2 and similar to the rate difference observed for Fe(CN)<sub>6</sub><sup>3-/4-</sup> and CPZ. A much larger difference was observed for Fe<sup>3+/2+</sup>, with  $k^0$  on PPF being a factor of 32 slower than that on HT GC and both being slower than  $k^0$  on polished GC ( $1.7 \times 10^{-3} \text{ cm/s}$ ). As stated earlier, Fe<sup>3+/2+</sup> electron transfer on carbon electrodes is catalyzed by surface carbonyl groups.<sup>39,40</sup> The lower O/C ratio on both HT GC and PPF results in slow electron transfer, resulting from the lack of catalytic carbonyl groups. The slower ET for Fe<sup>3+/2+</sup> on PPF compared to HT GC can possibly be due to the difference in the surface oxygen functionalities though there is no direct evidence to support this contention. Dopamine oxidation and O<sub>2</sub> reduction are known to involve reactant adsorption to the electrode surface, and their kinetics are significantly slower if such adsorption is intentionally blocked.<sup>31,43-46</sup> The slower DA and O<sub>2</sub> kinetics observed on PPF are consistent with the weaker MB adsorption discussed above. For reasons that are not yet clear, PPF interacts more weakly than HT GC with DA and O<sub>2</sub>, thus decreasing the catalytic effect of the carbon surface. The significant difference in  $\Delta E_p$  observed for DA between HT GC and PPF is too large (>200 mV) to be explained by the difference in roughness factor.

To confirm that internal resistance contributes to  $\Delta E_p$  values observed for PPF on silicon, a few electrodes were prepared by forming PPF on polished GC instead of silicon. After the same pyrolysis procedure, the PPF/GC surfaces appeared identical to PPF/Silicon, with the surface Raman spectrum clearly indicating that PPF had covered the GC substrate. The capacitance (9  $\mu\text{F}/\text{cm}^2$ ) and MB adsorption (20 pmol/cm<sup>2</sup>) of PPF on GC were very

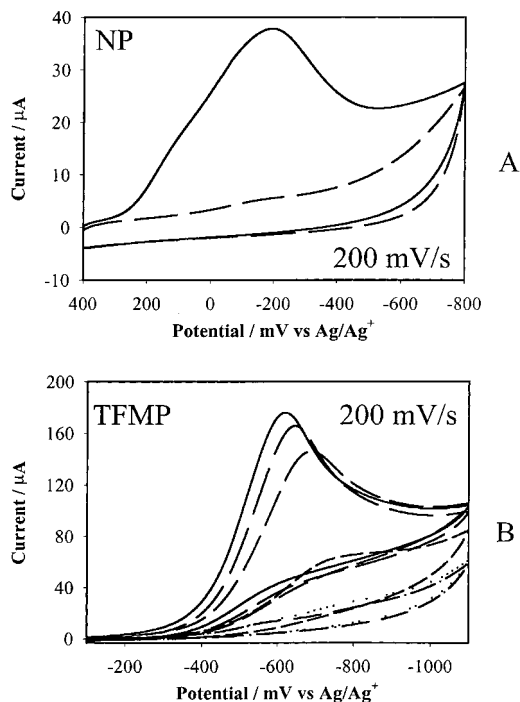


Figure 4. Cyclic voltammograms of nitrophenyl (A) and trifluoromethylphenyl (B) diazonium ions on PPF in 0.1 M TBABF<sub>4</sub> in acetonitrile. Both diazonium salts had bulk concentrations of 5 mM. The largest voltammetric current was observed on the first scan, then decreased with successive scans, as shown.

close to those on PPF/Si. The observed  $\Delta E_p$  values for the GC substrate are included in Table 3. For the outer-sphere redox systems (Ru(NH<sub>3</sub>)<sub>6</sub><sup>3+/2+</sup> and chlorpromazine), the PPF/GC results are similar to heat-treated GC, since there is little or no contribution from internal electrode resistance. This observation confirms that the electron-transfer rates for outer-sphere systems are very similar on PPF and heat-treated GC and that resistance in the thin film of PPF on silicon contributes significantly to potential error. For systems that depend strongly on surface interactions (e.g., DA, Fe<sup>3+/2+</sup>), the kinetics are determined by surface composition, and the substrate resistance has minor effects on  $\Delta E_p$ . For example, both DA and Fe<sup>3+/2+</sup> are much slower on PPF than on bare GC, due to differences in surface chemistry. However, the substrate for PPF has little effect on  $\Delta E_p$  for these systems (within experimental error), indicating that a contribution to  $\Delta E_p$  from resistance is minor compared to the kinetic effect.

**Surface Modification.** Chemical modification of carbon surfaces by electrochemical reduction of aromatic diazonium salts<sup>26,27</sup> was attempted on PPF films. A variety of carbon surfaces have been successfully modified with a compact monolayer of aryl groups covalently attached to the surface,<sup>27-31</sup> and this method of surface modification can result in electrodes with tailor-made properties. Surface modification of PPF was achieved by electrochemical reduction of nitrophenyl (NP) and trifluoromethyl (TFMP) diazonium salts in acetonitrile during cyclic voltammetry, as reported elsewhere.<sup>27,44</sup> Other diazonium salts used successfully include 4-nitrozobenzene (NAB) and 2-anthraquinone (2AQ). The potential was cycled between +0.4 and -0.8 V (NP) and -0.1 and -1.1 V (TFMP) until the reduction current became negligible and only the background current remained, as shown in Figure 4. For NP, the second cycle showed negligible reduction current,

(44) DuVall, S. H.; McCreery, R. L. *Anal. Chem.* **1999**, *71*, 4594.

(45) Xu, J.; Huang, W.; McCreery, R. L. *J. Electroanal. Chem.* **1996**, *410*, 235.

(46) Yang, H.-H.; McCreery, R. L. *J. Electrochem. Soc.* **2000**, *147*, 3420-3428.

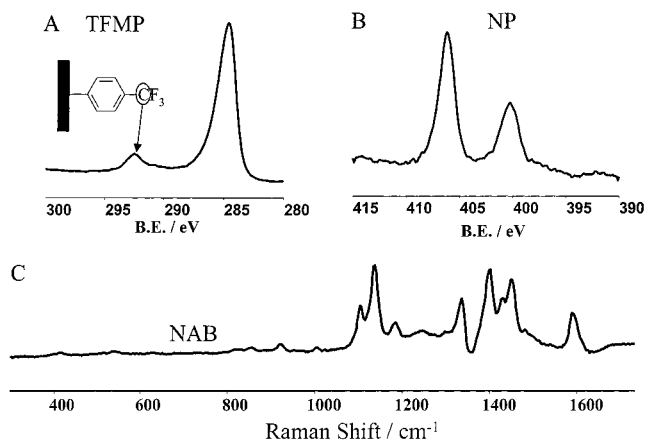


Figure 5. (A) XPS spectrum in the  $C_{1s}$  region of PPF following TFMP modification. (B) XPS spectrum in the  $N_{1s}$  region of PPF following NP modification. (C) Raman spectrum of nitroazobenzene-modified PPF after subtraction of PPF spectrum. Laser wavelength was 514.5 nm, and the integration time was 15 s.

and for TFMP, five cycles were required. The CVs are similar to those observed on GC, with a rapid decrease in reduction current as a monolayer is formed. To ensure the completion of derivatization, the electrodes were cycled for at least three more times after the reduction current had become negligible. After modification, the surfaces were thoroughly cleaned by sonication in AC/IPA solution followed by Nanopure water, to remove residual physisorbed materials. The NP-, NAB-, and TFMP-derivatized PPF surfaces were probed with XPS and Raman spectroscopy. Cyclic voltammetry of a chemisorbed 2AQ-derivatized surface shows the redox wave of the quinone group centered at  $-0.16$  V vs Ag/AgCl, verifying the presence of the electroactive 2AQ on the surface. Parts A and B of Figure 5 show the XPS  $C_{1s}$  region of 4-TFMP-derivatized PPF and  $N_{1s}$  region of 4-NP-derivatized PPF, respectively. Figure 5C shows the Raman spectra of NAB-modified PPF, after subtracting the PPF Raman spectrum. A comparison to previously published spectra for GC after reduction of these diazonium salts confirms the successful covalent modification of PPF surfaces.<sup>27,30</sup> The surface coverage was estimated by XPS as described elsewhere.<sup>30</sup> The estimated surface coverage for NP-, NAB-, and TFMP-modified PPF surfaces are 434, 276, and 411 pmol/cm<sup>2</sup>, respectively. This compares favorably with values reported earlier for glassy carbon and BDD surfaces.<sup>27,30</sup> Although PPF exhibits relatively weak physisorption of MB, the results of diazonium reduction indicate that covalent modification is both possible and favorable.

## DISCUSSION

Fabrication of small or complex carbon electrode configurations from PPF has been demonstrated elsewhere, and applications as LC detectors and ring-disk electrode analogues have been proposed.<sup>20–23</sup> Since the bulk and surface properties of carbon materials have pronounced effects on their suitability as electrodes, it is important to assess their electroanalytical properties. The focus of the current work is characterization of PPF in the context of common carbon electrode materials, particularly smoothness, background current, electron-transfer kinetics, surface oxide level, and stability. Although PPF is similar in many ways to a smooth version of polished glassy carbon, there are

some significant differences which may have substantial electroanalytical consequences. First, PPF is extraordinarily smooth, with a rms roughness approximately 1–10% of polished GC. Combined with the ability to produce patterns on a scale of 10–20  $\mu\text{m}$ , the flatness of PPF may permit fabrication of novel electrode structures such as interdigitated carbon arrays and very thin electrolyte layers. Second, the capacitance and background current are lower than GC, due to both a low roughness factor and possibly electronic effects (see below). Low background current may be quite valuable for trace analysis with voltammetry or LC/EC. Third, physisorption of methylene blue and AQDS is weak on PPF, much weaker than on polished or heat-treated GC. Fourth, electron-transfer rates are slightly slower for outer-sphere redox systems on PPF, but much slower for systems dependent on surface oxides or adsorption (e.g., DA,  $\text{Fe}^{3+/2+}$ ). The resistivity of PPF is quite close to that of GC, but significant internal resistance was observed for thin PPF films on silicon. For sensors and LC detectors operating at low current, the film resistance is likely to be negligible, even for quite small microstructures. Finally, the ability to form covalently bonded monolayers on the flat PPF surface opens the possibility of making microstructurally ordered arrays on carbon surfaces, analogous to the widely studied self-assembled monolayers on gold electrodes.

While the unusual properties of PPF may have practical value in electroanalytical applications, there is an important fundamental question about the relative influence of bulk and surface properties to PPF behavior. Some of the observations, such as low capacitance and weak adsorption can be partially explained by surface effects such as low roughness factor and low O/C ratio. It might be argued that GC 20 and PPF have similar or identical bulk properties, and the observed differences arise from the effects of heat treatment in an  $\text{H}_2$  atmosphere. The fact that the PPF resistivity is only slightly higher than GC 10 or GC 20 implies that the majority of changes in bulk electronic structure occur at heat treatment temperatures below 1000  $^\circ\text{C}$ . Without a direct measure of the bulk electronic properties of PPF compared to GC, such as the electronic density of states, it is difficult to determine whether PPF and GC differ in more than their surface properties.

Reported roughness factors for polished GC 20 are in the range of 1.5–2.5, so roughness could account for much of the factor of 2–4 higher capacitance and adsorption of heat-treated GC compared to PPF. Another factor of possible importance is the carbon microstructure near the PPF surface. Since GC is cured under high pressure and PPF is not, the graphitic regions may order differently as they are formed. It is possible that the edge/basal ratio of PPF is lower than GC, leading to lower capacitance and possibly lower adsorption.

## CONCLUSIONS

Pyrolyzed photoresist films have several electrochemical characteristics in common with conventional glassy carbon but have extremely flat surfaces ( $\sim 0.5$  nm rms). The low capacitance and weak adsorption properties of PPF are attractive features for electroanalytical applications. In addition, PPF may be fabricated lithographically into possibly complex microstructures or in unusual shapes that are not amenable to polishing. Since polishing

is unnecessary, mass production of PPF-based sensors is feasible. For outer-sphere redox systems, the resistance-corrected electron-transfer rates observed on PPF and GC are comparable, but for systems catalyzed by a surface interaction, PPF can be much less reactive than polished or heat-treated GC. The decreased electrocatalytic activity of PPF appears to stem from its low roughness factor, low oxide level, and possibly a lower percentage of basal plane on its surface. Although many of the differences between PPF and GC are attributable to differences in surface composition and roughness, the possibility that PPF and GC differ in their bulk electronic structure cannot be ruled out. At least for outer-

sphere redox systems such as  $\text{Ru}(\text{NH}_3)_6^{3+/2+}$  and CPZ, PPF and GC have similar electron-transfer reactivity.

#### ACKNOWLEDGMENT

The authors thank Surface and Analytical Chemistry Division of National Science Foundation for funding, and Marc Madou for useful suggestions and comments during the course of this work.

Received for review June 30, 2000. Accepted December 5, 2000.

AC0007534